Acta Geodyn. Geomater., Vol. 15, No. 3 (191), 297–309, 2018
DOI: 10.13168/AGG.2018.0022
journal homepage: https://www.irsm.cas.cz/acta

ORIGINAL PAPER

WEATHERING BY DOLOMITE DISSOLUTION RESPONSIBLE FOR THE FORMATION OF AN IMPORTANT PALAEOTOLOGICAL LOCALITY IN THE PRAGUE SYNFORM

Matt ROWBERRY [1)]*, Caroline DUBOIS [2)], Olivier KAUFMANN [2)], Jean-Marc BAELE [2)] and Jan BLAHŮT [1)]

[1)] *Department of Engineering Geology, Institute of Rock Structure & Mechanics ASCR, V Holešovičkách 41, 18209 Prague 8, Czech Republic*

[2)] *Department of Geology & Applied Geology, Faculty of Engineering, Université de Mons, 9, rue de Houdain, B-7000 Mons, Belgium*

**Corresponding author's e-mail:* rowberry@irsm.cas.cz

ARTICLE INFO

Article history:
Received 20 December 2017
Accepted 27 September 2018
Available online 4 October 2018

Keywords:
Carbonate rock weathering index
Polarising light microscopy
Cathodoluminescence microscopy
Calcite dissolution
Dolomite dissolution
Lower Devonian
Slivenec Limestone
Prague Synform

ABSTRACT

Karst landforms can result from a single stage process in which chemical dissolution and mechanical erosion proceed simultaneously or from a two stage process in which chemical dissolution precedes mechanical erosion. During the second of these processes, chemical dissolution leads to the creation of karst features hosting a residual weathering product, here referred to as alterite. An example of one such feature is the enclosed mass of altered rock at Červený Quarry near Klukovice which represents one of the richest localities for exceptionally preserved echinoderm ossicles in the Prague Synform. In this study the processes responsible for the formation of this feature have been investigated. Nineteen samples were obtained from the bioclastic Slivenec Limestone and from these it has been possible to calculate the carbonate volume content, which defines the weathering intensity, and the carbonate rock weathering index, which defines the weathering state. The results demonstrate that carbonate dissolution has not been accompanied by gravitational compaction or the incorporation of mineral inputs. Thin sections analysed under polarised light and under cathodoluminescence emphasise heterogeneous dolomitisation of the limestone. As the weathering grade intensifies, empty rhomboidal pores become increasingly common until, ultimately, the rhomboidal forms are lost due to corrosion and enlargement. In contrast it is rare to find evidence of calcite dissolution and, therefore, the altered mass still hosts almost all of its post dolomitisation micrite, sparite, and bioclasts. Negligible calcite dissolution helps to explain the exceptional nature of the fossil preservation at the site while the dolomite dissolution accounts for the ease with which it is possible to extract the fossils. Further research should focus on better understanding the role of dolomite dissolution in the formation of other important palaeontological localities in the Prague Synform.

1. INTRODUCTION

Limestones are dominated by the carbonate minerals calcite and aragonite, which represent different crystal forms of calcium carbonate, along with dolomite while less common minerals include ankerite, magnesite, and siderite (Fookes and Hawkins, 1988). Chemical interactions between fluids and minerals occur as a result of chemical disequilibria. Dissolution occurs when fluids are undersaturated with respect to some minerals, i.e. the equilibrium constant is greater than the ionic activity product (Noiriel et al., 2009). Carbonate mineral dissolution is particularly rapid in comparison to silicate and aluminosilicate mineral dissolution and, therefore, these minerals are the first to be modified in the presence of acidic fluids (Noiriel et al., 2005). Dissolution affects the micritic constituents of limestone more rapidly than it affects the sparitic constituents because the micritic constituents have a greater reactive surface area (Roques and Ek, 1973). Indeed micrite grains can be viewed as spheres whose radius decreases during dissolution while the sparite crystals can be viewed as volumes surrounding spherical pores whose radii are increasing (Noiriel et al., 2009). Limestone dissolution affects those parts of the rock characterised by the highest pore connectivity while the rate of dissolution reflects changes in the reactive surface area (Noiriel et al., 2009). Recent integrated experimental and modelling approaches have shown that the presence of silicates in limestone leads to heterogeneous dissolution at the microscale despite the fact that homogeneous dissolution is observed at the sample scale (Noiriel et al., 2013).

Most karst landforms are interpreted to have developed as a result of simultaneous limestone dissolution and mechanical erosion - this single stage process of landform development can be referred to as karstification by total removal (Quinif, 2010). However, in certain instances, it can be demonstrated that limestone dissolution and mechanical erosion are

Cite this article as: Rowberry M, Dubois C, Kaufmann O, Baele J-M, Blahůt J: Weathering by dolomite dissolution responsible for the formation of an important palaeotological locality in the Prague Synform.. Acta Geodyn. Geomater., 15, No. 3 (191), 297–309, 2018. DOI: 10.13168/AGG.2018.0022

sequential rather than simultaneous - this two stage process of landform development can be referred to as ghost rock karstification (Quinif et al., 2014). During the first stage, limestone dissolution, beginning with the micritic constituents and progressing to the sparitic constituents, leads to the formation of a karst feature hosting a predominantly insoluble material (Dubois et al., 2014a). During the second stage, this insoluble material, referred to as residual alterite, is subjected to mechanical erosion which leads to the creation of typical karst landforms such as caves, dolines, and poljes (Dubois et al., 2014a). In terms of the thermodynamic regime the first stage requires enough hydrodynamic energy to renew the acidic fluids while second stage requires enough hydrodynamic energy to remove the altered material (Quinif, 1998). Consequently the amount of hydrodynamic energy needed for this two stage process is considerably less than that needed for simultaneous limestone dissolution and mechanical erosion (Quinif et al., 2014). Transition from the first stage to the second stage may not occur for millions or hundreds of millions of years if, for example, the alterite is sealed during a marine transgression (Quinif et al., 2006).

Karst features hosting residual alterite are routinely exposed during limestone quarrying. Moreover, artificial quarry dewatering creates the hydrodynamic potential needed to mechanically erode the residual alterite and, therefore, it has been possible to experimentally observe the rapid transition from karst feature to karst landform (e.g. Quinif and Maire, 2009). Examples of the two stage process of ghost rock karstification have been reported from across Europe. In Belgium, instances have been described from, for example, the province of Hainaut (e.g. Dubois et al., 2014b) and the province of Liège (e.g. Dupont et al., 2018) while in France instances have been described from, for example, the region of Bourgogne Franche Comté (e.g. Barriquand et al., 2012), the region of Nouvelle Aquitaine (e.g. Dandurand et al., 2014), and the region of Occitanie (e.g. Bruxelles and Wienin, 2009). Notable examples have also been described from other parts of Europe including the Alps (e.g. Audra et al., 2007) and the United Kingdom (e.g. Rowberry et al., 2014). Similar ideas have also been expressed as a result of detailed studies in Slovenia (e.g. Zupan-Hajna, 2003). In this paper a case study is presented which investigates the formation of an enclosed mass of porous, altered limestone exposed in the western face of Červený Quarry near Klukovice. The palaeotological significance of this feature lies in the fact that it represents one of the richest localities for exceptionally preserved echinoderm ossicles in the Prague Synform.

2. GEOLOGICAL SETTING

The NE-SW striking Prague Synform extends from southwestern Prague to the Beroun District of Central Bohemia (Figure 1a-b). This synform hosts a range of fold structures including symmetrical, asymmetrical, and overturned folds while disharmonic folding often appears to reflect lithological contrasts between thick bedded, competent, and shale rich, incompetent, limestones (Chlupáč et al., 1998). Despite more than one hundred years of scientific debate no consensus has yet been reached regarding its origin (cf. Melichar, 2004; Röhlich, 2007). The majority of exposures in this area indicate marine deposition from the Lower Ordovician to the Middle Devonian. The Lower to Middle Devonian sequence is dominated by two groups of carbonate facies: the

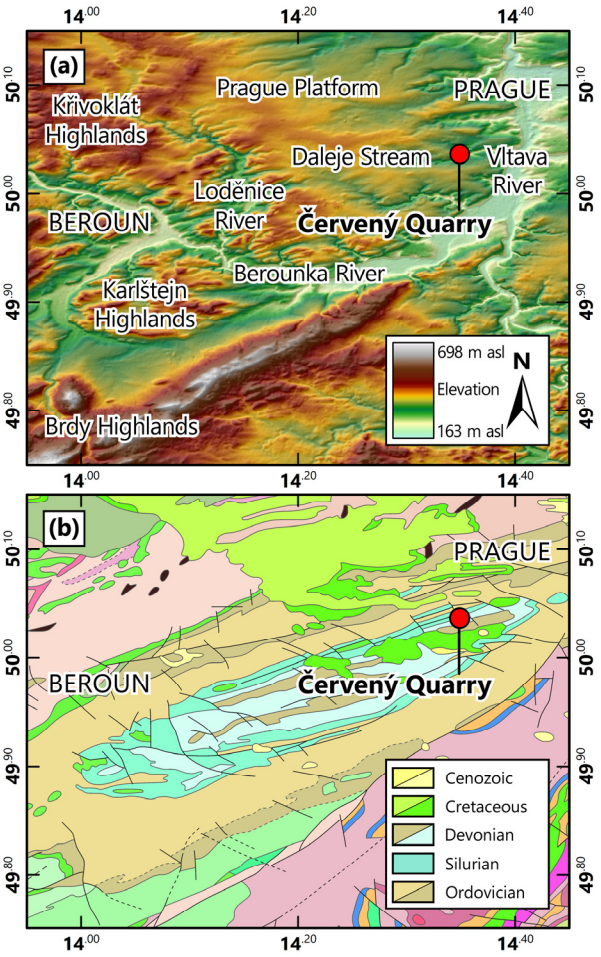

Fig. 1 (a) Topographic map showing the main rivers, e.g. the Vltava and Berounka Rivers, and geomorphological units, e.g. the Prague Platform and Brdy Highlands, together with the administrative centres of Prague and Beroun and the location of Červený Quarry near Klukovice; (b) Geological map of the region based on the 1:500 000 map published by the Czech Geological Survey (Cháb et al., 2007). For more detailed information, the website of the Czech Geological Survey hosts interactive maps at a scale of 1:50 000, with Červený Quarry located on sheet GM 12-42 (http://mapy.geology.cz/).

first are bioclastic and biolithic sediments deposited in comparatively shallow, high energy settings while the second are micritic and biomicritic sediments deposited in comparatively deep, low energy settings. It is common for shale and limestone layers to alternate (Chlupáč et al., 1998). During the Eifelian carbonate sedimentation was superseded by the deposition of calcareous shales and siliclastic sediments - this change represents the first manifestation of the Variscan Orogeny. Two postorogenic sequences are also found in the vicinity of the synform: the freshwater Upper Carboniferous sequence is dominated by coarse grained conglomerates and sandstones with subordinate fluvial and lacustrine clays while the Cretaceous sequence is characterised by sandy and clayey lacustrine sediments together with glauconitic sandstones and calcareous siltstones deposited in shallow epicontinental seas. Both sequences are thought to have once covered far larger areas than indicated by their present outcrops (Chlupáč, 1993).

The Lower Palaeozoic sequences of the Prague Synform form a region referred to as the Bohemian Karst. Limestones occur, either at the surface or at depth, over a total area of 144 km^2 (Žák et al., 2016). This region has remained emergent for protracted periods spanning from the Variscan Orogeny to the Cenomanian and from the Turonian to the Holocene. Prior to the Quaternary two periods are thought to have been particularly important for the development of karst features (Bosák et al., 1993): extensive depressions and underground drainage systems originated during the early Cretaceous (Bosák et al., 1989) while intensive karstification and weathering occurred during the late Cretaceous and Palaeogene (Bosák, 1990). It has been proposed that many of the karst features which developed during the early Cretaceous were reactivated during the late Cretaceous and Palaeogene (Cílek et al., 1995). Caves tend to be associated with steeply dipping traverse faults striking N-S or NW-SW although some systems have developed parallel to bedding or in association with disharmonic folding (Žák et al., 2016). Calcite veining across the region provide evidence for several phases of postorogenic hydrothermal circulation but the timing of these events remains poorly constrained (Suchý et al., 2000). The extensive Upper Cretaceous and Palaeogene denudation surface began to be entrenched by allochthonous rivers during the Oligocene and Miocene but this process intensified close to the transition from the early to middle Pleistocene (Tyráček et al., 2004). During this period a number of caves developed on the sides of the narrow valleys as a result of floodwater injection (Vysoká et al., 2012).

The limestones of the Bohemian Karst host one unusual feature of particular significance in the context of the present study, referred to locally as "white beds". These beds comprise laterally impersistent porous, altered limestones which, despite their name, may be whitish, greyish, yellowish, brownish, pinkish, or reddish (Petr et al., 1997). Scientific interest in the white beds stems primarily from the fact that they host huge numbers of exceptionally well preserved echinodermal ossicles, whose stereoms are of great importance for palaeobiology. The beds can be studied in a number of artificial and natural exposures around the Prague Synform and they may be *in situ*, i.e. white beds *sensu stricto*, or they may have been redeposited, i.e. white beds *sensu lato* (Suchý, 2002). The most easily accessible white bed localities are exposed in abandoned quarries along the Daleje and Prokop Valleys in the southwestern part of Prague (Martínková, 1997). Other significant sites are situated at greater depths such as the white beds exposed in Portálová Cave near Tetín (Žák et al., 2001). However, the deepest localities are only known from boreholes, with several instances reported hundreds of metres below the present surface (Ovčarov, 1972). It is commonly accepted that these beds result from chemical dissolution of the fresh limestone but the precise mechanisms remain enigmatic. The main hypotheses postulate, first, that the beds result from a process termed intergranular corrosion (Cílek et al., 1995) or, second, that they result from processes relating to the formation of carbonate soils (Suchý, 2002). It is interesting to note that descriptions of the intergranular corrosion process are markedly similar to descriptions of the ghost rock karstification process outlined in the introduction.

3. STUDY SITE

Červený Quarry near Klukovice is situated on the left side of the Daleje Stream, close to its confluence with the Prokop Stream which, in turn, represents a left hand tributary of the Vltava River. Quarrying began here in the early 1800s and stopped in the middle of the 1900s. During this period the excavated limestone was used both for the production of lime and as a local building material (Kříž, 1999). Červený Quarry, together with the neighbouring homestead of Opatřilka, was granted protected status as a natural monument in September 1982. The site covers a total area of 8.2 ha and spans elevations from 244 m asl to 318 m asl. It hosts flora and fauna typical of dry grasslands and species diversity is maintained through a grazing management program (Dostálek and Frantík, 2012). The faces of Červený Quarry expose sedimentary lithologies spanning from the uppermost Lochkovian to the lowermost Zlíchovian, a regional substage of the Emsian (Fig. 2). The Lochkov Formation is represented by the shallow water, i.e. benthic assemblage 2 or 3, light grey bioclastic sparry Kotýs Limestone (Chlupáč et al., 1998). The Praha Formation is represented by the shallow water, i.e. benthic assemblage 3, reddish to whitish bioclastic crinoidal Slivenec Limestone, the shallow water, i.e. benthic assemblage 3, multicoloured biomicritic to finely bioclastic Loděnice Limestone, the deep water,

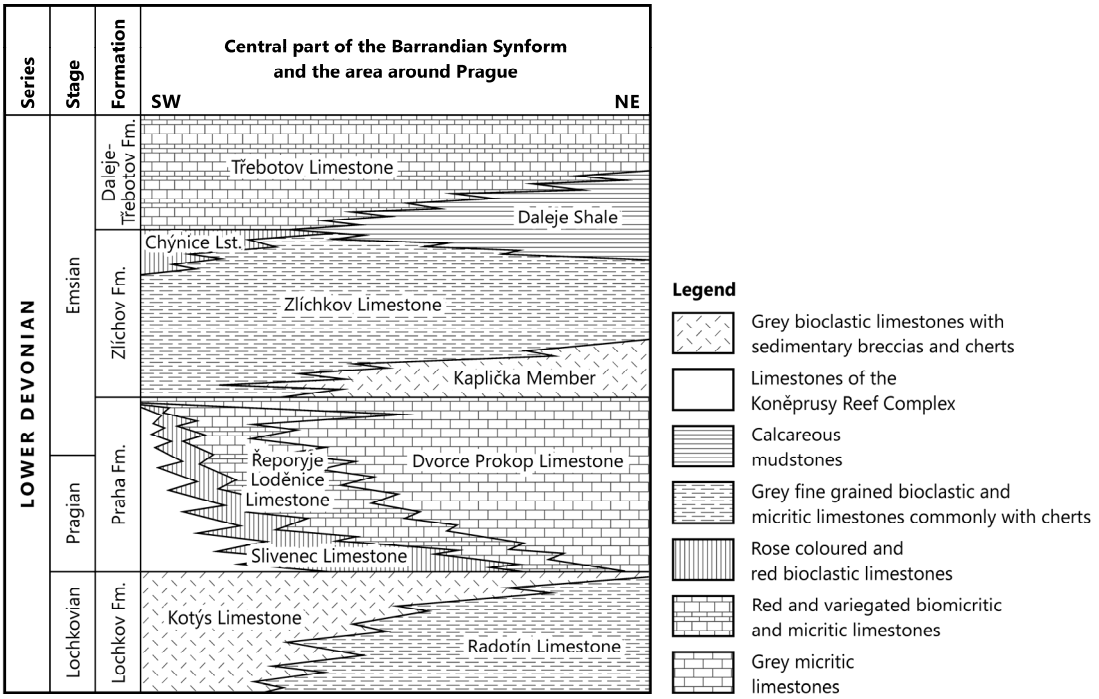

Fig. 2 Stratigraphic chart of the Lower Devonian of the Prague Synform based on Chlupáč et al. (1998) and modified from Budil et al. (2009). The faces of Červený Quarry expose the Kotýs Limestone, the Slivenec Limestone, the Řeporyje Limestone, the Dvorce-Prokop Limestone, and the Kaplička Member. The studied porous, altered mass has developed in the reddish to whitish bioclastic Slivenec Limestone (Praha Formation, Pragian, Lower Devonian).

i.e. benthic assemblage 4 to 5, reddish to purplish micritic or biomicritic nodular Řeporyje Limestone, and the deep water, i.e. benthic assemblage 4 to 5, light grey micritic or biomicritic nodular or platy Dvorce and Prokop Limestones (Chlupáč et al., 1998). The Zlíchov Formation is represented by the Kaplička Member - this is an intraformational breccia with bioclastic limestone which gradually passes upwards into a micritic platy limestone (Chlupáč et al., 1998). The geological and palaeontological significance of this protected area is illustrated by the broad range of scientific topics that have been addressed using samples from the site (e.g. Frýda et al., 2013; Holcová and Slavík, 2013; Hunter and McNamara, 2017).

4. METHODS

From a theoretical perspective, limestones and dolostones comprise a void phase, $j = 0$, a soluble phase, $j = 1$, and, commonly, an insoluble phase, $j = 2$ (Fig. 3a). The soluble phase is represented by carbonate minerals and the insoluble phase is represented by silicate and aluminosilicate minerals. Weathering can be described by one of four petrophysical models, two of which introduce a mineral input phase, $j = 3$ (Dubois et al., 2015). In the first model, weathering reflects dissolution of the soluble phase, but no other processes are involved (Fig. 3a). In the second model, weathering reflects dissolution of the soluble phase accompanied by gravitational compaction (Fig. 3c). In the third model, weathering reflects dissolution of the soluble phase accompanied by the incorporation of mineral inputs (Fig. 3d). In the fourth model, weathering reflects dissolution of the soluble phase accompanied by gravitational compaction and the incorporation of mineral inputs (Fig. 3e). It can be seen that weathering in the first and third models is isovolumetric whereas weathering in the second and fourth models is not isovolumetric due to the gravitational compaction.

Theoretical laws have been established for each of these petrophysical models in order to relate a small number of measureable rock properties to the recently proposed carbonate rock weathering index (Dubois et al., 2015). The carbonate rock weathering index represents a universal mathematical protocol which is able to define the weathering state completely independently of the specific processes involved in the weathering. This is often necessary in geotechnical engineering and, therefore, the carbonate rock weathering index represents an important alternative to traditional assessments based on macroscopic descriptions of particular rock properties including colour, structure, and friability (Price, 2009). To determine which petrophysical model is most appropriate for a given sample it is only necessary to measure its porosity, density, and carbonate mass fraction. Then on the basis of these three measureable rock properties it is possible to calculate its carbonate

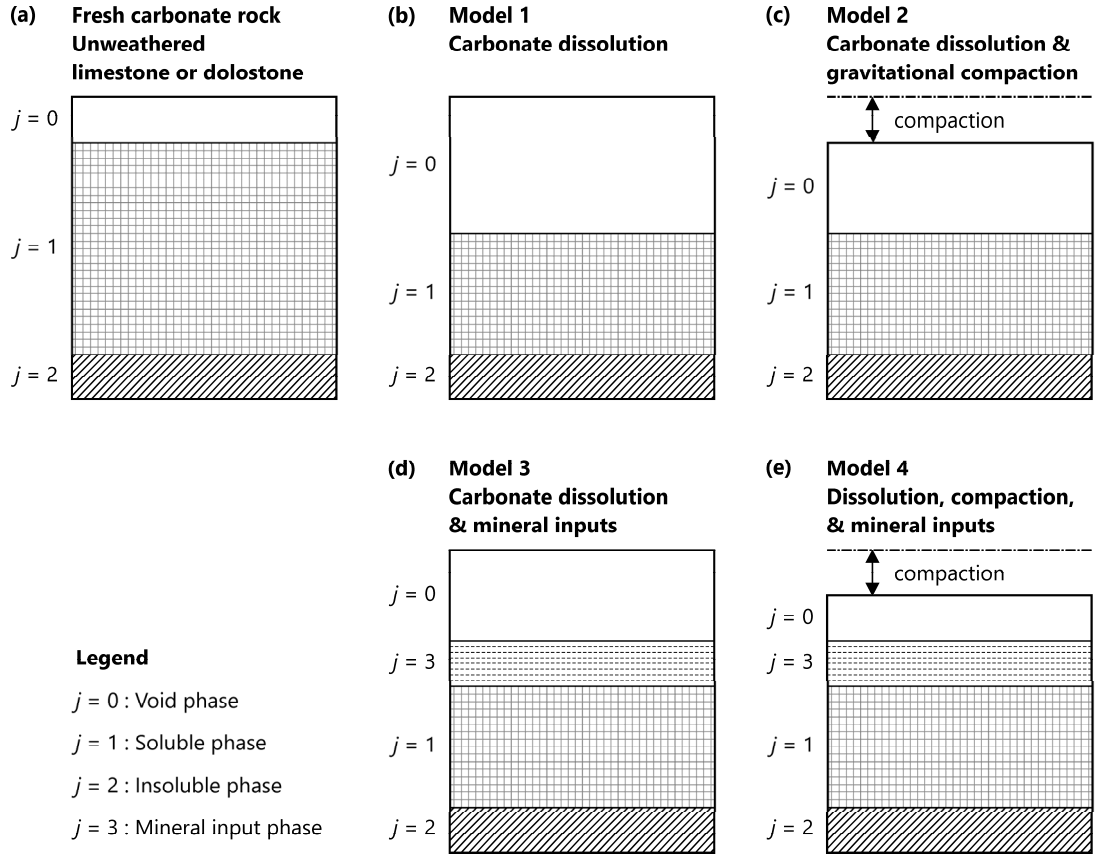

Fig. 3 Petrophysical models outlining the main processes involved in the weathering of carbonate rocks: (a) fresh unweathered limestone or dolostone comprising a void phase, a soluble phase, and an insoluble phase; (b) weathering reflects dissolution of the soluble phase; (c) weathering reflects dissolution of the soluble phase and gravitational compaction; (d) weathering reflects dissolution of the soluble phase and the incorporation of mineral inputs; (e) weathering reflects dissolution of the soluble phase, gravitational compaction, and the incorporation of mineral inputs (modified from Dubois et al., 2015).

volume content and carbonate rock weathering index. Detailed descriptions of the mathematical protocol and analytical procedures used to determine the measurable rock properties are outlined elsewhere (Dubois, 2015).

In Červený Quarry the steeply dipping, buckled strata of the Slivenec Limestone host an enclosed mass of porous, altered rock through which it is possible to trace the original bedding (Fig. 4). Unfortunately this outcrop has not attracted much sedimentological and mineralogical attention but a detailed microfacies analysis of the Slivenec Limestone has been made at Cikánka in the nearby Radotín Valley (Čáp et al., 2003). There the limestone is associated with abundant crinoids, brachiopods, and trilobites as well as common ostracodes and tentaculites. In addition dolomite is also abundant while micrite and sparite are common and clay and pyrite are rare (Čáp et al., 2003). In Červený Quarry a total of nineteen samples were collected from seven strata: at least two samples were obtained from each stratum, one representing fresh limestone and one representing its altered counterpart. In each case, on the basis of its macroscopic properties, the lowermost

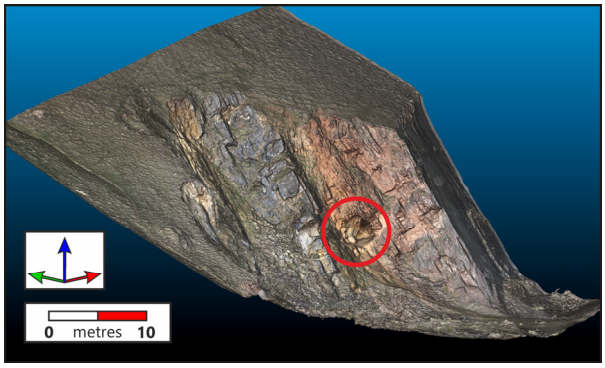

Fig. 4 3D surface model of the western face of Červený Quarry generated using a digital camera mounted on an unmanned aerial vehicle (Balek and Blahůt, 2017). The steeply dipping, buckled strata of the Slivenec Limestone hosts an enclosed mass of altered rock, indicated by the circle.

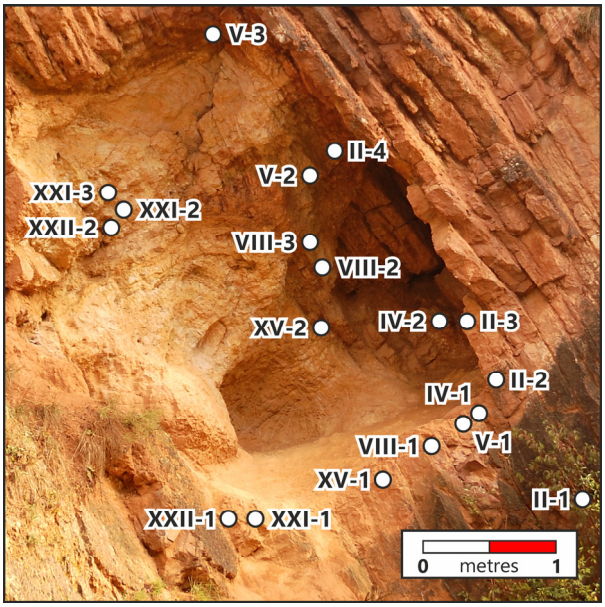

Fig. 5 Field photograph of the enclosed mass of altered rock situated in the Slivenec Limestone at Červený Quarry. The positions of the nineteen sampling points are labelled but the individual stratum, particularly those at its base, are concealed by sediments recently washed out of the cavity. On the basis of their macroscopic properties it was anticipated that the lowermost sample from each stratum would represent fresh limestone.

sample from each stratum was expected to represent fresh limestone (Fig. 5).

To calculate the density of each sample, its mass was determined using a set of precision scales and its global volume was determined using a carbon volumeter. Its density was then defined by Equation 1:

$$\gamma_r = \frac{M_{tot}}{V_{tot}} \tag{1}$$

Where: M_{tot} represents the mass of each sample and V_{tot} represents its global volume. To calculate the porosity of each sample, its global volume was determined using a volumeter while its volume without voids was determined using a helium pycnometer. Its porosity was then defined by Equation 2:

$$v_0 = \frac{V_{tot} - V_{rock}}{V_{tot}} \tag{2}$$

Where: V_{tot} represents the global volume of each sample and V_{rock} represents its volume without voids. To calculate the carbonate mass content of each sample, the carbonate content was determined by measuring its rate of response to dilute hydrochloric acid using a Dietrich-Frühling Calcimeter. Its carbonate mass content was then defined by Equation 3:

$$m_{CO_3^{2-}} = \frac{M_{CO_3^{2-}}}{M_{tot}} \tag{3}$$

Where: $M_{CO_3^{2-}}$ represents the carbonate content of each sample and M_{tot} represents its total mass. The carbonate volume content of each sample was determined on the basis of its density and carbonate mass content. This is defined by Equation 4:

$$v_{CO_3^{2-}} = \frac{m_{CO_3^{2-}} \cdot \gamma_r}{\gamma_{CO_3^{2-}}} \tag{4}$$

Where: $m_{CO_3^{2-}}$ represents the carbonate mass content of each sample, γ_r represents its density, and $\gamma_{CO_3^{2-}}$ is assumed to be equal to the density of calcite (2.71 g/cm³). The carbonate rock weathering index of each sample was determined on the basis of its carbonate volume content and the carbonate volume content of fresh rock. This is defined by Equation 5:

$$RWI = 1 - \frac{CO_3^{2-}\ volume\ content\ of\ the\ sample}{CO_3^{2-}\ volume\ content\ of\ the\ fresh\ rock} \tag{5}$$

For completely unweathered rock the carbonate rock weathering index will equal 0 while for fully weathered rock the carbonate rock weathering index will equal 1 (Dubois et al., 2015).

Thin sections have been prepared from four samples, spanning from fresh rock to intensively weathered, so as to better understand the weathering process, or processes, and to investigate the effect of the weathering on the microstructure of the rock. Slivers of fresh rock could be mounted directly on glass slides while the weathered samples had to be vacuum impregnated with epoxy resin prior to cutting, mounting, and polishing. A Leica DMLP petrographic microscope has been used to analyse the thin sections under plane and cross polarised light while a CITL Mk5 CL stage operating at 15 kV and 500 µA has been used to analyse the thin sections under cathodoluminescence. Once the main luminescence centres in the carbonates, e.g. Mn^{2+} substituting for Ca^{2+} and Mg^{2+}, have been excited by a beam of electrons, calcite minerals often luminesce brown or yellow to orange while dolomite often glow bright red (Machel, 2000).

5. RESULTS

5.1. CALCULATING THE CRWI

The density measurements range from a minimum of 1.31 g/cm^3 to a maximum of 2.74 g/cm^3 as presented in Table 1 and Figure 6a, the porosity measurements range from a minimum of 0.6 % to a maximum of 53 % as presented in Table 2

Table 1 The density measurements obtained from samples of fresh limestone and their altered counterparts (g/cm³).

Sample	*II*	*IV*	*V*	*VIII*	*XV*	*XXI*	*XXII*
1	2.74	2.70	2.65	2.68	1.64	2.56	2.20
2	2.64	2.60	1.31	2.53	2.01	1.44	1.52
3	1.79		2.24	2.16		1.48	
4	2.32						

Table 2 The porosity measurements obtained from samples of fresh limestone and their altered counterparts (%).

Sample	*II*	*IV*	*V*	*VIII*	*XV*	*XXI*	*XXII*
1	0.6	2.2	4.4	5.2	41.8	9.3	20.7
2	2.7	4.6	52.6	10.2	27.4	49.5	49.3
3	34.8		19.4	25.0		49.3	
4	17.2						

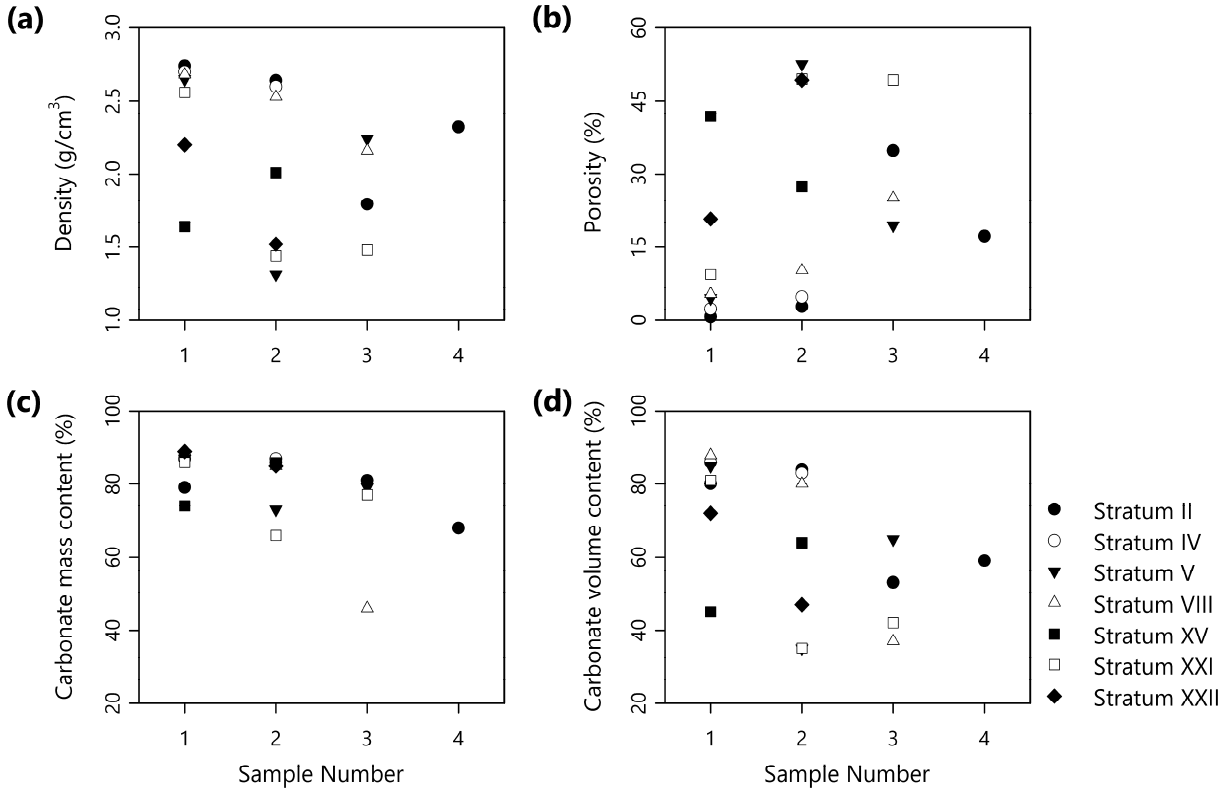

Fig. 6 (a) Densities of the fresh limestone and their altered counterparts in each stratum; (b) Porosities of the fresh limestone and their altered counterparts in each stratum; (c) Carbonate mass content of the fresh limestone and their altered counterparts in each stratum; (d) Carbonate volume content of the fresh limestone and their altered counterparts in each stratum.

and Figure 6b, the carbonate mass content measurements range from a minimum of 46 % to a maximum of 89 % as presented in Table 3 and Figure 6c, and the calculated carbonate volume content ranges from a minimum of 35 % to a maximum of 88 % as presented in Table 4 and Figure 6d. It is clear that the samples of supposedly fresh limestone have all been affected by alteration to a greater or lesser extent, with the least weathered limestone represented by the lowermost sample from Stratum VIII and the most weathered limestone represented by samples from Stratum V and Stratum XXI. It can be seen that density and porosity develop in an entirely consistent manner while the carbonate mass content does not develop in a manner consistent with density and porosity.

The carbonate volume content calculated for each sample is plotted against their density measurements in Figure 7a, their porosity measurements in Figure 7b, and their carbonate mass content measurements in Figure 7c. The carbonate volume content is a reflection of the weathering intensity - the sample with the greatest volume is that which has been least affected by alteration. If the

Table 3 The carbonate mass content measurements obtained from samples of fresh limestone and their altered counterparts (%).

Sample	*II*	*IV*	*V*	*VIII*	*XV*	*XXI*	*XXII*
1	79	87	87	89	74	86	89
2	86	87	73	85	86	66	85
3	81		79	46		77	
4	68						

Table 4 The carbonate volume content calculated from samples of fresh limestone and their altered counterparts (%).

Sample	*II*	*IV*	*V*	*VIII*	*XV*	*XXI*	*XXII*
1	80	86	85	88	45	81	72
2	84	83	35	80	64	35	47
3	53		65	37		42	
4	59						

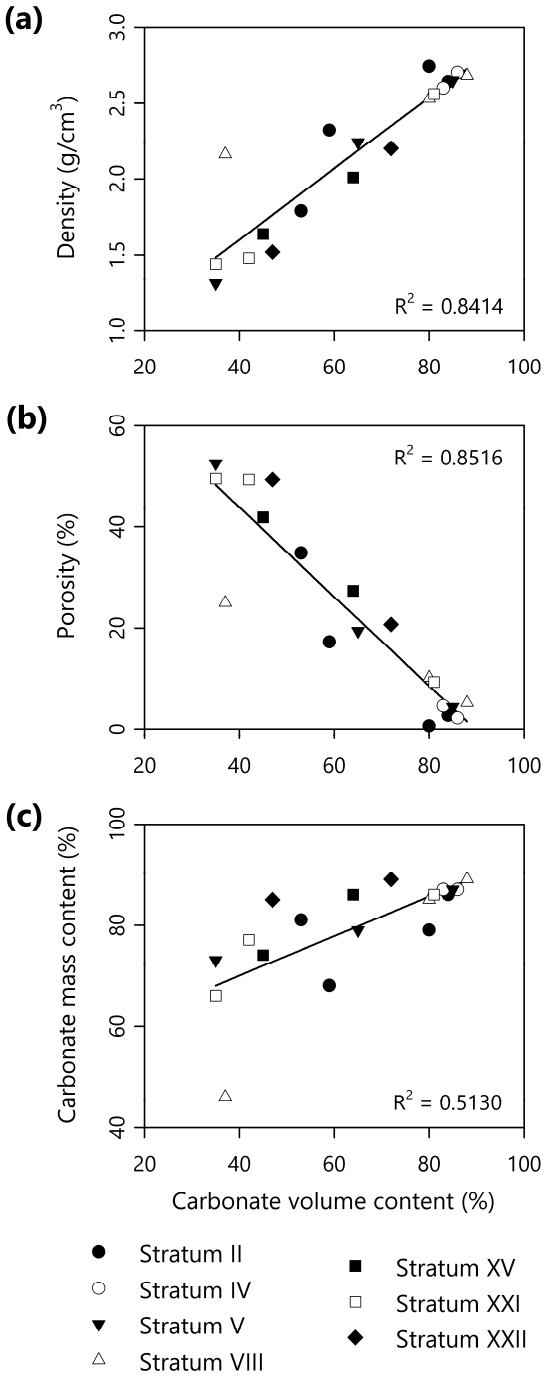

Fig. 7 (a) The density of each sample plotted against its carbonate volume content; (b) The porosity of each sample plotted against its carbonate volume content; (c) The carbonate mass content of each sample plotted against its carbonate volume content.

alteritic mass developed in a manner consistent with the simplest weathering scenario, i.e. the alterite reflects only the process of carbonate dissolution without significant gravitational compaction or the incorporation of mineral inputs, it follows that there should be linear relationships between, first, the density measurements and their carbonate volume content and, second, the porosity measurements and their carbonate volume content. It can be seen that both the density and porosity measurements follow consistent linear trends with respect to their carbonate volume content. This demonstrates that the weathering process reflects only the process of carbonate dissolution.

The carbonate rock weathering index calculated for each sample, presented in Table 5, is plotted against their density measurements in Figure 8a, their porosity measurements in Figure 8b, and their carbonate mass content measurements in Figure 8c. Unfortunately it has not been possible to calculate the weathering index for each stratum as not all the strata provided a sample of fresh limestone. However, it is reasonable to assume that the initial properties of the fresh limestone in each stratum were approximately the same and, therefore, these properties are likely to be well represented by the lowermost sample from Strata XIII. It can be seen that both the density and porosity measurements follow consistent linear trends with respect to their carbonate rock weathering index although the trends are opposing, i.e. the positive correlation between density and carbonate volume content is negative between density and the carbonate rock weathering index.

Table 5 The carbonate rock weathering index calculated from samples of fresh limestone and their altered counterparts (%).

Sample	*II*	*IV*	*V*	*VIII*	*XV*	*XXI*	*XXII*
1	10	2	4	0	49	8	18
2	5	5	60	10	28	60	46
3	39		26	58		52	
4	34						

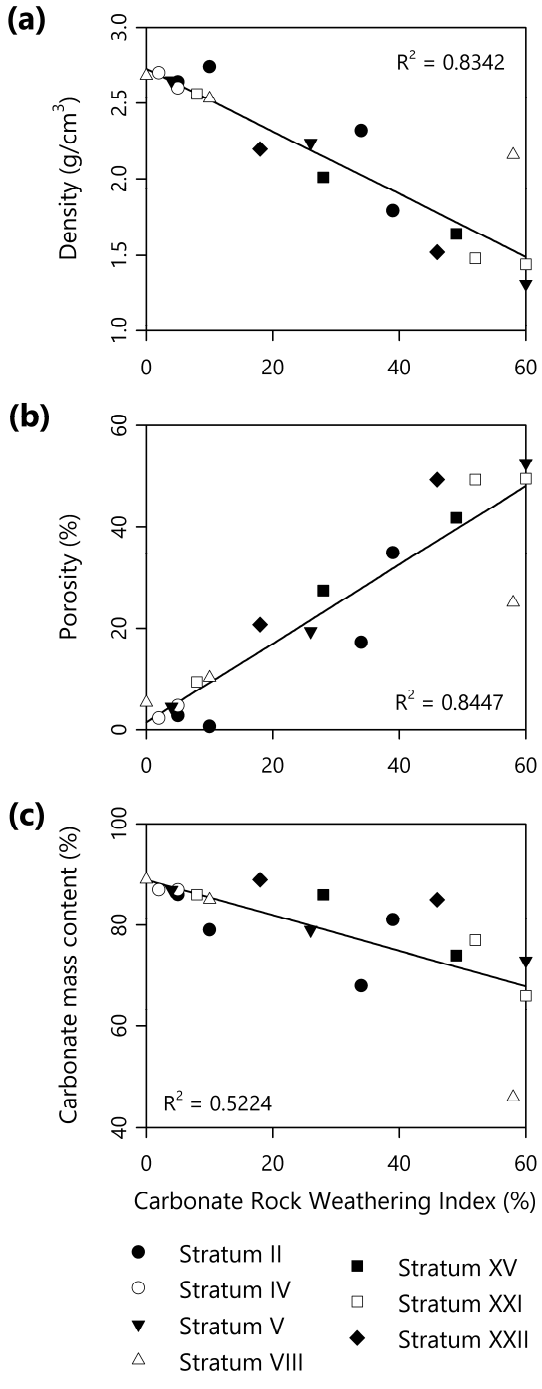

Fig. 8 The density of each sample plotted against its carbonate rock weathering index; (B) The porosity of each sample plotted against its carbonate rock weathering index; (C) The carbonate mass content of each sample plotted against its carbonate rock weathering index.

5.2. THIN SECTION ANALYSIS

Four samples have been studied under polarised light and under cathodoluminescence: fresh rock is represented by Sample II-1; slightly weathered rock is represented by Sample II-3; moderately weathered rock is represented by Sample II-4; and intensively weathered rock is represented by Sample VIII-3. The fresh limestone is fine grained with occasional floating bioclasts. At the microscopic scale it can be seen that this limestone is heterogeneously dolomitised, from a few vol. % to nearly 100 vol. %, while individual dolomite rhombs have diameters of approximately 50 μm. Iron oxide staining is common in the intergranular space between dolomite rhombs (Figs. 9a-d). The slightly weathered limestone is not thought to have ever been dolomitised to the same extent as its fresh counterpart. However, empty rhomboidal pores are reasonably common, their shape indicating that the rock has been affected by dolomite dissolution. Dolomite calcitisation, a process referred to as dedolomitisation, is observed in exceptional cases (Figs. 9e-f). The moderately weathered limestone is also not thought to have ever been dolomitised to the same extent as its fresh counterpart. Once again, empty rhomboidal pores are reasonably common, but here there is also evidence of calcite dissolution, most especially at contacts between calcite veins and fine grained matrix although calcite dissolution is also recognised within individual veins (Figs. 9g-h). The intensively weathered limestone appears to have been dolomitised to a similar extent as the fresh limestone. Not only has dissolution excavated the dolomite rhombs but the rhomboidal shape of the empty pores has been lost due to corrosion and enlargement. It is estimated that the porosity of this limestone, at least locally, may be as great as 50 %. The rims of the pores are coated with a clayey iron oxide material and this is interpreted to be the same as that observed in the fresh rock (Figs. 9i-j). No evidence for syntaxial overgrowth has been observed in any of the thin sections.

6. DISCUSSION

Limestones and dolostones represent particularly challenging foundation materials as their dissolution has the potential to greatly modify stability of the rock mass and its hydrological behaviour (Fookes and Hawkins, 1988). The carbonate rock weathering index represents a universal mathematical protocol for defining the weathering state completely

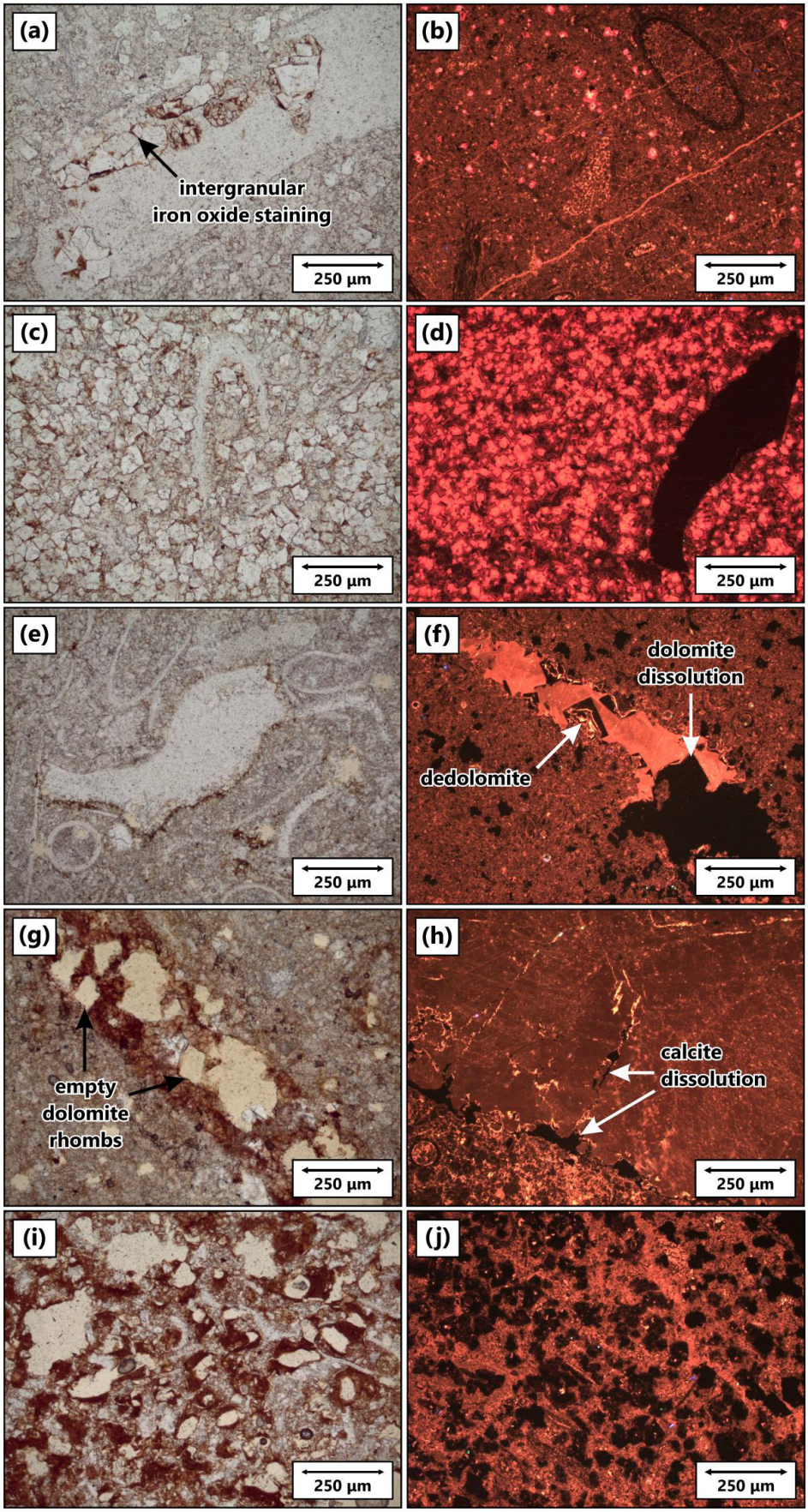

Fig. 9 Thin section analysis of the Slivenec Limestone at Červený Quarry under polarised light, left hand column, and under cathodoluminescence, right hand column: (a-d) Micrographs of the fine grained fresh limestone which demonstrate heterogeneous dolomitisation and iron oxide staining in the intergranular space between dolomite rhombs; (e-f) Micrographs of the slightly weathered limestone which demonstrate the presence of empty rhomboidal pores and only exceptional instances of dedolomitisation; (g-h) Micrographs of the moderately weathered limestone which demonstrate instances of calcite dissolution at contacts between calcite veins and the fine grained matrix; (i-j) Micrographs of the intensively weathered limestone which demonstrate corrosion and enlargement of the empty rhomboidal pores as well as the presence of iron oxide staining around the pore rims. Calcite minerals luminesce brown to yellow to orange while dolomite minerals luminesce bright red. The beige colour of the voids under polarised light reflects minor burning of the epoxy resin while under cathodoluminescence.

independently of the specific processes involved in the weathering. On the basis of this information it is then possible to assess changes to the mechanical and hydrological properties of the rock as weathering proceeds (Dubois et al., 2015). As the mathematical protocol is neither site dependent nor operator dependent, it is thought that this approach represents a significant advance on traditional geotechnical assessments of the weathering state, which are usually based on macroscopic descriptions of specific rock properties. Nonetheless it has been stressed that the modelled outputs should be analysed critically to ensure that they are consistent with field observations (Dubois et al., 2015). In this study the carbonate rock weathering index has been tested on an experimental dataset obtained from an important palaeotological site in the Prague Synform. It is the first time that the mathematical protocol has been applied outside the Carboniferous Limestone of southern Belgium and it is also the first time that the protocol has been applied to samples containing potentially significant – but unknown – amounts of dolomite.

The Carboniferous Limestone of southern Belgium has long been known to host numerous karst features filled with residual alterite. This alterite results from calcite dissolution and may be subjected to gravitational compaction and the incorporation of mineral inputs and, therefore, the mathematical protocol emphasises the importance of these processes. However, it is possible that calcite dissolution does not represent the most important weathering process in dolomitised rocks, so it important to assess whether the theoretical and methodological approaches are robust. In the petrophysical models, the soluble phase does not differentiate between calcite dissolution and dolomite dissolution and, therefore, it is more appropriate to refer to *carbonate dissolution* rather than *calcite dissolution*, sensu Dubois et al. (2015). Regarding the measurable parameters, care must be taken to ensure that the calcimetric measurements account for both the fast reacting calcite minerals and the slow reacting dolomite minerals. If this condition is met, then it is appropriate to replace the term *calcite mass content* with *carbonate mass content*, and it follows that it is necessary to replace the term *calcite volume* with *carbonate volume content*. These changes are also reflected in the equations as $CaCO_3$ has been replaced by CO_3^{2-}. On these grounds it can be concluded that the mathematical protocol is robust for both limestones and dolostones.

Thin sections were prepared in order to understand the importance of calcite dissolution relative to the importance of dolomite dissolution. From these it can be seen that dolomite dissolution has been fundamental to the formation of the porous, altered mass at Červený Quarry. Due to their rhomboidal shape, the empty pores are interpreted to result from the local dissolution of metastable dolomite minerals and, as such, the dissolution process appears to be fundamentally unrelated to the dolomitisation process. On the basis that a number of calcite veins in this area were precipitated from shallower meteoric waters, it is suggested that the oldest conceivable age for dolomite dissolution is contemporaneous with the most recent phase of calcite veining in the Prague Synform (Suchý et al., 2000). The fact that the pores are usually empty - dedolomite is only observed in exceptional cases - points to a much more recent age although, as dolostone loses its porosity at a slower rate than limestone, it is possible for pore space to be preserved during deep burial. Calcite dissolution has not been fundamental to the formation of this altered mass but future changes in the mechanical and hydrological properties of the mass could be caused by calcite dissolution. The structural integrity of the residual alterite is indicated by the fact that the thermodynamic regime has not imparted enough energy to cause its mechanical erosion - the cavity itself has formed as a result of fossil hunting excavations.

Neither ideas relating to the theory of ghost rock karstification nor ideas relating to the formation of the white beds can be reconciled easily with the presented results. In both cases, calcite dissolution is assumed to be the dominant weathering process – in the Czech literature this is referred to as intergranular corrosion (e.g. Cílek et al., 1995) or intergranular karstification (e.g. Bosák, 1996). In ghost rock karstification it is assumed that the residual alterite comprises a predominately insoluble material but this is clearly not the case at Červený Quarry. Here the residual alterite has lost much of its dolomite but it still comprises almost all of its micrite, sparite, and bioclasts. Weathering by dolomite dissolution explains the ease with which it is possible to extract the fossils from the site while negligible calcite dissolution explains the exceptional nature of the fossil preservation. Further research should focus on better understanding the role of dolomite dissolution in the formation of other important palaeontological localities in the Prague Synform. This is not suggested in any of the existing published literature but there is some circumstantial evidence to support the hypothesis: no typical karst landforms are found along the Daleje and Prokop Valleys, which suggests the impotence of calcite dissolution hereabouts, yet these valleys still host a number of white bed localities (Martínková, 1997).

7. CONCLUSIONS

In this study it has been possible to investigate the processes responsible for the formation of an enclosed mass of altered rock at Červený Quarry near Klukovice. This feature represents one of the richest localities for exceptionally preserved echinoderm ossicles in the Prague Synform. In total nineteen samples were obtained from the reddish to whitish

bioclastic crinoidal Slivenec Limestone. On the basis of three measureable parameters it has been possible to calculate the carbonate volume content and carbonate rock weathering index for each sample. These results demonstrate that carbonate dissolution at the site has not been accompanied by gravitational compaction or the incorporation of mineral inputs. On the basis of thin section analysis under polarised light and under cathodoluminescence it has been possible to better understand the weathering process. These results demonstrate heterogeneous dolomitisation of the limestone. As the weathering grade intensifies, empty rhomboidal pores become increasingly common until, ultimately, the rhomboidal forms are lost due to corrosion and enlargement. In contrast it is rare to find indications of calcite dissolution and, therefore, the altered mass still hosts almost all of its micrite, sparite, and bioclasts. No evidence for syntaxial overgrowth has been observed in any of the thin sections. Negligible calcite dissolution helps to explain the exceptional nature of the fossil preservation at the site while the dolomite dissolution accounts for the ease with which it is possible to extract the fossils. Further research should focus on better understanding the role of dolomite dissolution in the formation of other important palaeontological localities in the Prague Synform.

ACKNOWLEDGEMENTS

The authors would like to thank Karel Žák and Václav Suchý for their insightful and constructive reviews which helped to greatly improve parts of the manuscript. This study has been conducted with support from the long term conceptual development research organisation RVO: 67985891. Financial assistance was provided by a research grant from the Institute of Rock Structure & Mechanics ASCR (ÚSMH Project 503-15).

REFERENCES

Audra, P., Bini, A., Gabrovšek, F., Häuselmann, P., Hobléa, F., Jeannin, P.-Y., Kunaver, J., Monbaron, M., Šušteršič, F., Tognini, P., Trimmel, H. and Wildberger, A.: 2007, Cave and karst evolution in the Alps and their relation to paleoclimate and paleotopography. Acta Carsologica, 36, 53–68. DOI: 10.3986/ac.v36i1.208

Balek, J. and Blahůt, J.: 2017, A critical evaluation of the use of an inexpensive camera mounted on a recreational unmanned aerial vehicle as a tool for landslide research. Landslides, 14, 1217–1224. DOI: 10.0.3.239/s10346-016-0782-7

Barriquand, L., Barriquand, J., Baele, J.-M., Dechamps, S., Guillot, L., Maire, R., Nykiel, C., Papier, S. and Quinif, Y.: 2012, The Caves of Azé (Saône-et-Loire, France). Karstologia, 59, 19–32, (in French).

Bosák, P.: 1990, Tropical paleokarst of the Bohemian Massif in Czechoslovakia. Studia Carsologica, 3, 19–26.

Bosák, P.: 1996, The evolution of karst and caves in the Koněprusy region (Bohemian Karst, Czech Republic) and paleohydrological model. Acta Carsologica, 25, 57–67.

Bosák, P., Cílek, V. and Bednářová, J.: 1993, Tertiary morphogeny and karstogenesis of the Bohemian Karst. Knihovna České speleologické společnosti, 21, 10–19.

Bosák, P., Horáček, I. and Panoš, V.: 1989, Paleokarst of Czechoslovakia. In: Bosák, P., Ford, D., Glazek, J. and Horáček, I. (Eds.) Paleokarst. Academia, Prague, 107–135.

Bruxelles, L. and Wienin, M.: 2009, The ghost rocks of the mine of La Grande Vernissière (Fressac, Gard). Karstologia Mémoires, 17, 192–200, (in French).

Budil, P., Hörbinger, F. and Mencl, R.: 2009, Lower Devonian dalmanitid trilobites of the Prague Basin (Czech Republic). Earth Env. Sci. T. R. So., 99, 2, 61–100. DOI: 10.1017/S1755691009006161

Čáp, P., Vacek, F. and Vorel, T.: 2003, Microfacies analysis of Silurian and Devonian type sections (Barrandian, Czech Republic). Czech Geological Survey, Special Paper, 15, 40 pp.

Cháb, J., Stráník, Z. and Eliáš, M.: 2007, Geological map of the Czech Republic 1:500 000. Czech Geological Survey, Prague.

Chlupáč, I.: 1993, Geology of the Barrandian. Senckenbergische Naturforschende Gesellschaft, Frankfurt am Main, 163 pp.

Chlupáč, I., Havlíček, V., Kříž, J., Kukal, Z. and Štorch, P.: 1998, Palaeozoic of the Barrandian (Cambrian to Devonian). Czech Geological Survey, Prague, 183 pp.

Cílek, V., Bosák, P. and Bednářová, J.: 1995, Intergranular corrosion, infiltrational kaolinization, and epigenetically reddened limestones of the Bohemian Karst, and their influence on karst morphology. Studia Carsologica, 6, 131–150.

Dandurand, G., Maire, R., Dubois, C. and Quinif, Y.: 2014, The Charente karst basin of the Touvre. Geologica Belgica, 17, 27–32.

Dostálek, J. and Frantík, T.: 2012, The impact of different grazing periods in dry grasslands on the expansive grass Arrhenatherum elatius L. and on woody species. Environ. Manage., 49, 855–861. DOI: 10.1007/s00267-012-9819-4

Dubois, C.: 2015, Effects of weathering phenomena on calcareous rocks: from rock to aquifer properties. PhD Thesis, Université de Mons, 376 pp.

Dubois, C., Deceuster, J., Kaufmann, O. and Rowberry, M.: 2015, A new method to quantify carbonate rock weathering. Math. Geosci., 47, 889–935. DOI: 10.1007/s11004-014-9581-7

Dubois, C., Quinif, Y., Baele, J.-M., Barriquand, L., Bini, A., Bruxelles, L., Dandurand, G., Havron, C., Kaufmann, O., Lans, B., Maire, R., Martin, J., Rodet, J., Rowberry, M., Tognini, P. and Vergari, A.: 2014a, The process of ghost rock karstification and its role in the formation of caves. Earth. Sci. Rev., 131, 116–148. DOI: 10.1016/j.earscirev.2014.01.006

Dubois, C., Quinif, Y., Baele, J.-M., Dagrain, F., Deceuster, J. and Kaufmann, O.: 2014b, The evolution of the mineralogical and petrophysical properties of a weathered limestone in southern Belgium. Geologica Belgica, 17, 1–8.

Dupont, N., Quinif, Y., Dubois, C., Cheng, H. and Kaufmann, O.: 2018, Karstic system of Sprimont (Belgium). Holotype of a speleogenesis by ghost rock karstification. Bulletin de la Société Géologique de France, 189, 1, 22 pp., (in French). DOI: 10.1051/bsgf/2017205

Fookes, P. and Hawkins, A.: 1988, Limestone weathering: its engineering significance and a proposed

classification scheme. Q. J. Eng. Geol. Hydroge., 21, 7–31. DOI: 10.1144/GSL.QJEG.1988.021.01.02

Frýda, J., Ferrová, L. and Frýdaová, B.: 2013, Review of palaeozygopleurid gastropods (Palaeozygopleuridae, Gastropoda) from Devonian strata of the Perunica microplate (Bohemia), with a re-evaluation of their stratigraphic distribution, notes on their ontogeny, and descriptions of new taxa. Zootaxa, 3669, 469–489. DOI: 10.11646/zootaxa.3669.4.3

Holcová, K. and Slavík, L.: 2013, The morphogroups of small agglutinated foraminifera from the Devonian carbonate complex of the Prague Synform, (Barrandian area, Czech Republic). Palaeogeogr.Palaeocl., 386, 210–224. DOI: 10.1016/j.palaeo.2013.05.022

Hunter, A. and McNamara, K.: 2017, Paleozoic echinoderm hangovers: waking up in the Triassic. Geology, 45, e431. DOI: 10.1130/G39575C.1

Kříž, J.: 1999, Geological Monuments of Prague. Czech Geological Institute, Prague, 280 pp., (in Czech).

Machel, H.: 2000, Application of cathodoluminescence to carbonate diagenesis. In: Pagel, M., Barbin, V., Blanc, P. and Ohnenstetter, D. (Eds.) Cathodoluminescence in Geosciences. Springer, Berlin, 271–301.

Martínková, M.: 1997, Geology and petrology of the so-called white beds in the Palaeozoic Barrandian. Diploma Thesis, Charles University in Prague, 88 pp., (in Czech).

Melichar, R.: 2004, Tectonics of the Prague Synform: a hundred years of scientific discussion. Krystalinikum, 30, 167–187.

Noiriel, C., Bernard, D., Gouze, P. and Thibault, X.: 2005, Hydraulic properties and microgeometry evolution accompanying limestone dissolution by acidic water. Oil Gas Sci. Technol., 60, 177–192. DOI: 10.2516/ogst:2005011

Noiriel, C., Gouze, P. and Madé, B.: 2013, 3D analysis of geometry and flow changes in a limestone fracture during dissolution. J. Hydrol., 486, 211–223. DOI: 10.1016/j.jhydrol.2013.01.035

Noiriel, C., Luquot, L., Madé, B., Raimbault, L., Gouze, P. and Van der Lee, J.: 2009, Changes in reactive surface area during limestone dissolution: an experimental and modelling study. Chem. Geol., 265, 160–170. DOI: 10.1016/j.chemgeo.2009.01.032

Ovčarov, K.: 1972, Evaluation of limestone and cement raw materials in the western part of the Barrandian. Geoindustria, Prague, 189 pp., (in Czech).

Petr, V., Prokop, R., Mihaljevič, M. and Šebek, O.: 1997, Chemical composition of the crinoid skeletal remains (Echinodermata) in weathered limestones of the Bohemian Lower Devonian (Barrandian area). J. Czech Geol. Soc., 42, 41–51.

Price, D.: 2009, Engineering Geology: Principles and Practice. Springer, Berlin, 450 pp.

Quinif, Y.: 1998, Dissipation of energy and adaptability in karst systems. Karstologia, 31, 1–11, (in French).

Quinif, Y.: 2010, Ghost rocks and phantomisation – essay on a new paradigm in karstogenesis. Karstologia Mémoires, 18, 184 pp., (in French).

Quinif, Y. and Maire, R.: 2009,[Quentin Cave (Hainaut, Belgium) - an evolutionary model of ghosts rocks. Karstologia Mémoires, 17, 214–218, (in French).

Quinif, Y., Baele, J.-M., Dubois, C., Havron, C., Kaufmann, O. and Vergari, A.: 2014, Ghost karstification theory - a new paradigm between Davis' two phase theory and Erhart's biorhexistasy theory. Geol. Belg., 17, 66–74, (in French).

Quinif, Y., Meon, H. and Yans, J.: 2006, Nature and dating of karst filling in the Hainaut Province (Belgium). Geodin. Acta, 19, 73–85. DOI: 10.3166/ga.19.73-85

Röhlich, P.: 2007, Structure of the Prague Basin. Bull. Geosci., 82, 175–182.

Roques, H. and Ek, C.: 1973, Experimental study of the dissolution of limestones by a water charged with CO_2. Ann. Spéléol., 28, 549–563, (in French).

Rowberry, M., Battiau-Queney, Y., Walsh, P., Błażejowski, B., Bout-Roumazeilles, V., Trentesaux, A., Křížová, L. and Griffiths, H.: 2014, The weathered Carboniferous Limestone at Bullslaughter Bay, South Wales: the first example of ghost-rock recorded in the British Isles. Geol. Belg., 17, 33–42.

Suchý, V.: 2002, The "white beds" - a fossil caliche of the Barrandian area. J. Czech Geol. Soc., 47, 45–54.

Suchý, V., Heijlen, W., Sýkorová, I., Muchez, P., Dobes, P., Hladíková, J., Jačková, I., Šafanda, J. and Zeman, A.: 2000, Geochemical study of calcite veins in the Silurian and Devonian of the Barrandian Basin (Czech Republic). Sediment. Geol., 131, 201–219. DOI: 10.1016/S0037-0738(99)00136-0

Tyráček, J., Westaway, R. and Bridgland, D.: 2004, River terraces of the Vltava and Labe (Elbe) system, Czech Republic, and their implications for the uplift history of the Bohemian Massif. Proc. Geol. Assoc., 115, 101–124. DOI: 10.1016/S0016-7878(04)80022-1

Vysoká, H., Bruthans, J., Žák, K. and Mls, J.: 2012, Response of karst phreatic zone to flood events in a major river (Bohemian Karst, Czech Republic) and its implication for cave genesis. J. Cave Karst Stud., 74, 65–81. DOI: 0.4311/2010ES0178R

Žák, K., Bosák, P. and Bruthans, J.: 2016, The Bohemian Karst. In: Pánek, T. and Hradecký, J. (Eds.) Landscapes and Landforms of the Czech Republic. Springer, Cham, 59–72. DOI: 10.1007/978-3-319-27537-6_6

Žák, K., Frýda, J., Bruthans, J., Kadlec, J. and Živor, R.: 2001, A new locality of "white beds" in Portálka Cave in the Kavčí (Montánka) Quarry near Tetín. Český kras, 27, 36–39, (in Czech).

Zupan-Hajna, N.: 2003, Incomplete Solution: Weathering of Cave Walls and the Production, Transport, and Deposition of Carbonate Fines. Karst Research Institute, Ljubljana, 167 pp.